Sensitivity Enhancement of Triple-Resonance Protein NMR Spectra by Proton Evolution of Multiple-Quantum Coherences Using a Simultaneous ^{1}H and ^{13}C Constant-Time Evolution Period

Zhigang Shang, G. V. T. Swapna, Carlos B. Rios, and Gaetano T. Montelione*

Contribution from the Center for Advanced Biotechnology and Medicine, and Department of Molecular Biology and Biochemistry, Rutgers University, Piscataway, New Jersey 08854-5638

Received March 6, 1997[⊗]

Abstract: Short transverse relaxation times of C^α and H^α single-quantum states in proteins reduce signal-to-noise ratios of heteronuclear correlation experiments involving transfers of C^α and H^α coherences. To overcome this "short transverse relaxation problem", we have developed a simultaneous ^{1}H and ^{13}C constant-time (sim-CT) heteronuclear multiple-quantum coherence (HMQC) scheme. New features in this design include: (i) utilization of heteronuclear multiple-quantum coherences for better transverse relaxation properties, (ii) concatenation of proton evolution into the simultaneous ^{1}H and ^{13}C constant-time period to eliminate separate time periods for proton evolution, and (iii) use of simultaneous ^{1}H and ^{13}C constant-time to remove resonance splitting due to multiple two- and three-bond homo- and heteronuclear scalar couplings. This general approach for sensitivity enhancement is demonstrated for the HA(CA)(CO)NH triple-resonance experiment. Results on proteins show that, compared with the heteronuclear single-quantum coherence version of the same experiment, on average the sim-CT HMQC version of HA(CA)-(CO)NH exhibits enhancements of ∼20%.

Introduction

Resonance assignments form the basis for interpreting multidimensional NMR spectra of proteins in terms of solution structure and dynamics.[1,2] The introduction of multi-dimensional triple-resonance NMR experiments has dramatically improved the speed and reliability of the assignment process.[3−10] Although these experiments have been successfully demonstrated with a large number of small proteins, for larger proteins, experiments involving magnetization transfer and frequency evolution of ^{1}H and ^{13}C nuclei with short transverse relaxation times become insufficiently sensitive. One approach to overcoming this "transverse relaxation problem" is utilization of ^{2}H,^{13}C,^{15}N -enriched samples in deuterium-decoupled triple-resonance experiments.[11−13] For ^{13}C,^{15}N -enriched proteins not enriched with deuterium, and for triple-resonance experiments utilizing indirect detection of aliphatic protons, another possible approach is to design pulse sequences involving multiple-quantum magnetization states during frequency evolution and coherence evolution periods. These multiple-quantum (MQ) coherences can exhibit better relaxation properties[14−19] than the corresponding single-quantum (SQ) magnetization states generally employed in triple-resonance experiments. Since transverse relaxation rates due to dipolar interactions are proportional to the square of nuclear gyromagnetic ratios, removal of the dipolar interaction of ^{1}H from the directly-bound ^{13}C nucleus can significantly decrease the transverse relaxation rate of ^{13}C. Of course, the dipolar interactions between protons can also effect ^{1}H−^{13}C multiple-quantum transverse relaxation rates, and the extent of improved relaxation rates will then depend on the local proton environment.[16,18] An additional potential drawback of using multiple-quantum states during indirect frequency evolution periods is that they are modulated by scalar coupling interactions with passive spins. This results in splittings in the indirect dimension which reduce the effective sensitivity and thus diminish the advantages of improved relaxation rates.[20] We have recently shown that these splittings due to homo- and heteronuclear two-bond and three-bond scalar couplings can be decoupled during an indirect-detection period using simultaneous proton and carbon constant-time heteronuclear multiple-quantum

* Author to whom correspondence should be addressed at the following: CABM, Rutgers University, 679 Hoes Lane, Piscataway, NJ 08854-5638; phone 908-235-5321; fax 908-235-4850; email guy@nmrlab.cabm.rutgers.edu.

⊗ Abstract published in *Advance ACS Abstracts,* September 15, 1997.

(1) Wüthrich, K. *NMR of Proteins and Nucleic Acids*; Wiley: New York, NY, 1986.
(2) Clore, G. M.; Gronenborn, A. M. *Science* **1991**, *252*, 1390−1399.
(3) Montelione, G. T.; Wagner, G. *J. Am. Chem. Soc.* **1989**, *111*, 5474−5475.
(4) Montelione, G. T.; Wagner, G. *J. Magn. Reson.* **1990**, *87*, 183−188.
(5) Ikura, M.; Kay, L. E.; Bax, A. *Biochemistry* **1990**, *29*, 4659−4667.
(6) Kay, L. E.; Ikura, M; Tschudin, R.; Bax, A. *J. Magn. Reson.* **1990**, *89*, 496−514.
(7) Kay, L. E.; Ikura, M.; Bax, A. *J. Magn. Reson.* **1991**, *91*, 84−92.
(8) Boucher, W.; Laue, E. D.; Campbell-Burk, S.; Domaille, P. J. *J. Am. Chem. Soc.* **1992**, *114*, 2262−2264.
(9) Bax, A.; Grzesiek, S. *Acc. Chem. Res.* **1993**, *26*, 131−138.
(10) Lyons, B. A.; Montelione, G. T. *J. Magn. Reson. B* **1993**, *101*, 206−209.
(11) Grzesiek, S.; Anglister, J.; Ren, H.; Bax, A. *J. Am. Chem. Soc.* **1993**, *115*, 4369−4370.
(12) Yamazaki, T.; Lee, W.; Revington, M.; Mattiello, D. L.; Dahlquist, F. W.; Arrowsmith, C. H.; Kay, L. E. *J. Am. Chem. Soc.* **1994**, *116*, 6464−6465.
(13) Farmer, B. T., II; Venters, R. A. *J. Am. Chem. Soc.* **1995**, *117*, 4187−4188.
(14) Ernst, R. R.; Bodenhausen, G.; Wokaun, A. *Principles of Nuclear Magnetic Resonance in One and Two Dimensions;* Clarendon Press: Oxford, England, 1987.
(15) Billeter, M.; Neri, D.; Otting, G.; Qian, Y. Q.; Wüthrich, K. *J. Biomol. NMR* **1992**, *2*, 257−274.
(16) Grzesiek, S.; Bax, A. *J. Biomol. NMR* **1995**, *6*, 335−339.
(17) Grzesiek, S.; Kuboniwa, H.; Hinck, A. P.; Bax, A. *J. Am. Chem. Soc.* **1995**, *117*, 5312−5315.
(18) Swapna, G. V. T.; Rios, C. B.; Shang, Z.; Montelione, G. T. *J. Biomol. NMR* **1997**, *9*, 105−111.
(19) Griffey, R. H.; Redfield, A. G. *Q. Rev. Biophys.* **1987**, *19*, 51−82.
(20) Boucher, W.; Laue, E. D.; Campbell-Burk, S. L.; Domaille, P. J. *J. Biomol. NMR* **1992**, *2*, 631−637.

S0002-7863(97)00734-8 CCC: $14.00

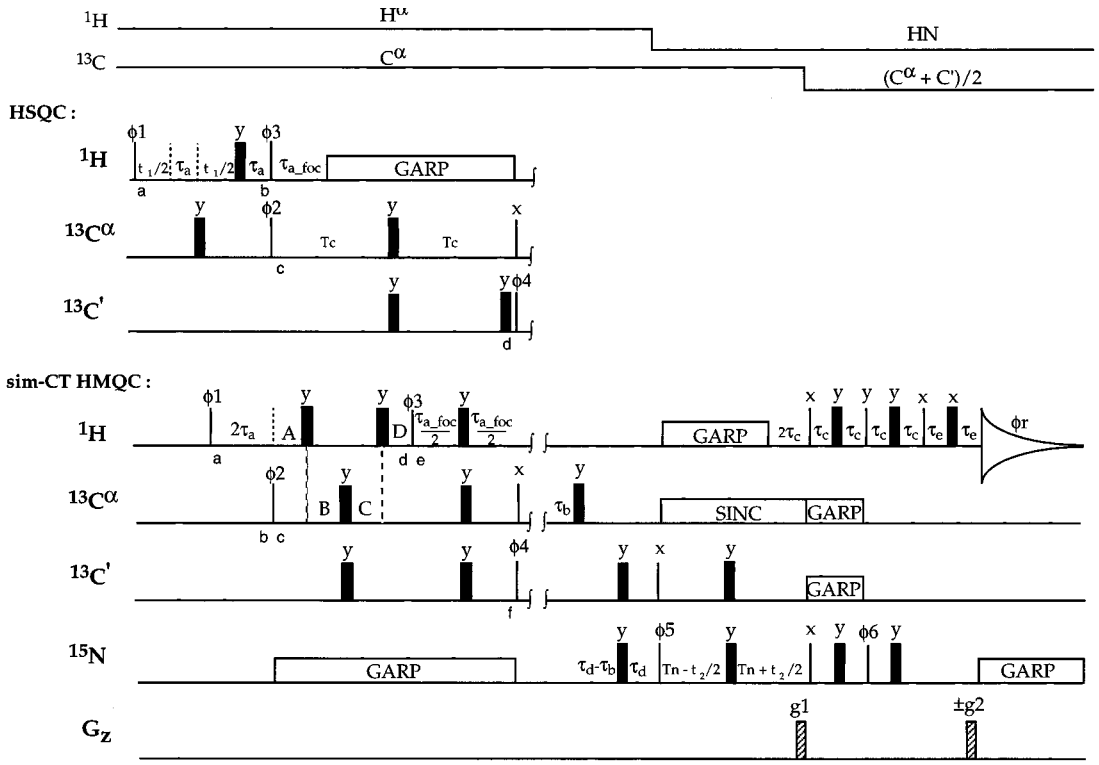

Figure 1. Pulse sequences of 3D HSQC- and sim-CT HMQC-HA(CA)(CO)NH experiments. Typical coherence transfer delays were tuned to $\tau_a = 1.6$ ms, $\tau_{a\_foc} = 2.3$ ms, $\tau_b = 3.5$ ms, $\tau_c = 2.8$ ms, $\tau_d = 15.0$ ms, and $\tau_e = 650$ μs, and the constant-times were set to $T_c = 4.2$ ms and $T_n = 13.5$ ms. During the constant-time $2T_c$ period, the ^{15}N spins were decoupled using GARP,[27] and during the constant-time $2T_n$ period, the $^{13}C^{\alpha}$ spins were decoupled using band-selective sinc wave forms. The pulse phases were cycled as follows: $\phi 2 = +x, -x$; $\phi 3 = 4(+y), 4(-y)$; $\phi 4 = +x, +x, -x, -x$; $\phi 5 = 8(+x), 8(-x)$. The receiver phase was cycled as follows: $\phi r = +x, -x, -x, +x, -x, +x, +x, -x, -x, +x, +x, -x, +x, -x, -x, +x$. The second carbonyl 180° pulse in the HSQC version pulse sequence is used to correct small phase shifts due to off-resonance effects. Quadrature detection in the t_1 dimension is obtained by changing the phase $\phi 1$ in the States-TPPI manner[28] and in the t_2 domain by inverting $\phi 6$ and the gradient g2 simultaneously as described by Kay *et al.*[29] Pulsed-field gradients are applied along the *z*-axis with an amplitude of ~28 G/cm and gradient durations g1 and g2 of ~5 and ~0.5 ms, respectively. These pulse sequences and decoupling wave forms are available by anonymous ftp from nmrlab.cabm.rutgers.edu or over the world-wide web at http://www-nmr.cabm.rutgers.edu.

coherence (HMQC), or sim-CT HMQC,[18] with chemical shift evolution of ^{13}C. For proteins in the molecular mass range of 6−16 kD, this approach results in average signal-to-noise (S/N) enhancements of 5% in sim-CT HMQC-type (HA)CANH and (HA)CA(CO)NH triple-resonance experiments compared with the corresponding heteronuclear single-quantum coherence (HSQC)-type versions of these experiments.

Several heteronuclear correlation experiments developed for macromolecules involving indirect proton frequency evolution suffer significant magnetization reductions because of the short transverse relaxation times of C^{α} and H^{α}. Having realized this problem, several groups[21,22] have introduced a semi-constant-time proton evolution, in which the INEPT transfer period is also used for proton frequency evolution, shortening the duration of transverse relaxation in the t_1 dimension by $(2J)^{-1}$. Sim-CT HMQC triple-resonance pulse sequences can also be designed with frequency-labeling of H^{α} (instead of C^{α}) during the indirect HMQC evolution period. This concatenates the proton frequency evolution period with the sim-CT HMQC period used for developing the required coherence transfers. In this study, we demonstrate this general approach for sensitivity enhancement in the design of an improved pulsed-field gradient (PFG) constant-time HA(CA)(CO)NH triple-resonance experiment,[8,23] in which the evolution of the $^1H^{\alpha}$ magnetization is incorporated into the simultaneous proton and carbon constant-time multiple-quantum period and the splittings due to all homo- and heteronuclear ^2J and ^3J scalar couplings are decoupled during the t_1 evolution period. The performance of HSQC and sim-CT HMQC versions of HA(CA)(CO)NH triple-resonance experiments are compared for the 124-residue bovine pancreatic ribonuclease A (RNase A) and 58-residue bovine pancreatic trypsin inhibitor (BPTI) proteins. Cross peak intensities in the sim-CT HMQC version experiment exhibit, on average, 20% enhancement compared with the corresponding HSQC version experiment.

Results and Discussion

The HA(CA)(CO)NH experiment[8,23] correlates the H^{α} resonance with sequential interresidue ^{15}N and H^N resonances. Shown in Figure 1 are HSQC and sim-CT HMQC versions of PFG-HA(CA)(CO)NH experiments. In the HSQC version experiment, the H^{α} transverse magnetization is frequency-labeled and subsequently developed into antiphase with respect to C^{α} via an INEPT transfer.[24] During the constant-time ($2T_c$) period, the C^{α} magnetization that is antiphase with respect to H^{α} is refocused into in-phase C^{α} magnetization and then developed into C^{α} magnetization that is antiphase with respect to C′. A replacement of the period described above by simultaneous H^{α} and C^{α} constant-time HMQC gives an improved pulse sequence, sim-CT HMQC HA(CA)(CO)NH, with significantly enhanced sensitivity.

The relevant magnetization transfer pathway between points a and f in Figure 1 is described in product operator

(21) Grzesiek, S.; Bax, A. *J. Biomol. NMR* **1993**, *3*, 185−204.
(22) Logan, T. M.; Olejniczak, E. T.; Xu, R. X.; Fesik, S. W. *J. Biomol. NMR* **1993**, *3*, 225−231.
(23) Feng, W.; Rios, C. B.; Montelione, G. T. *J. Biomol. NMR* **1996**, *8*, 98−104.
(24) Morris, G. A.; Freeman, R. *J. Am. Chem. Soc.* **1979**, *101*, 760−762.

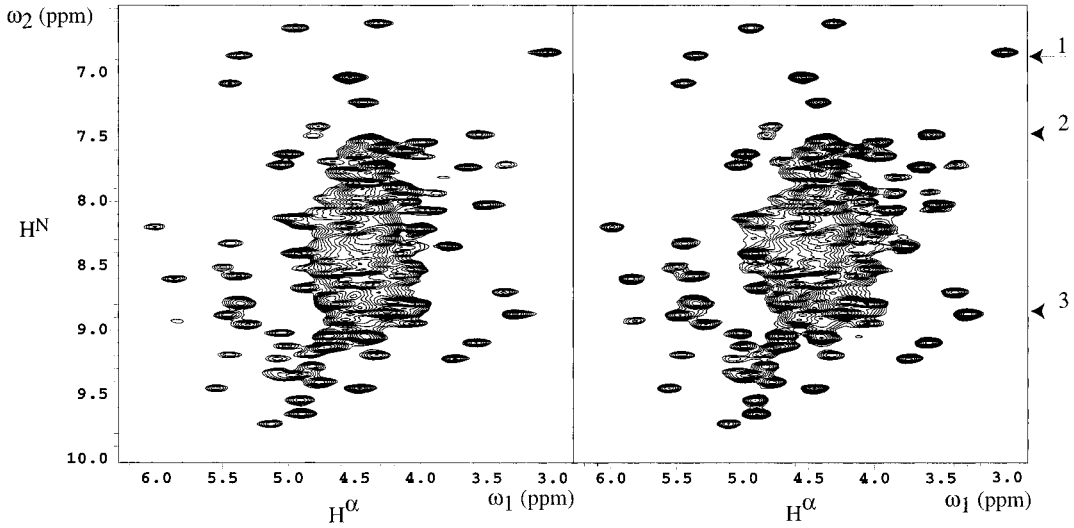

Figure 2. Comparison of H^N-H^α 2D spectra of $^{15}N,^{13}C$-enriched RNase A at 2 mM concentration, pH 4.6, and temperature of 20 °C generated with the two HA(CA)(CO)NH pulse sequences shown in Figure 1. For both data sets, the time domain data consisted of 42 and 1024 complex data points in t_1 and t_2, respectively, and the data in the t_1 dimension were extended to 84 points by linear prediction and zero-filled to 512 points prior to Fourier transformation. The HSQC (left) and sim-CT HMQC (right) spectra were recorded and processed under identical conditions and are plotted with the same vertical scale and apparent noise level. For each spectrum, 192 transients were acquired for each t_1 increment and the total collection time was ~7 h.

formalism[25]

$$H_z^\alpha \xrightarrow{a} -H_y^\alpha \xrightarrow{b} 2H_x^\alpha C_z^\alpha \xrightarrow{c} -2H_x^\alpha C_y^\alpha \xrightarrow{d} 4H_x^\alpha C_x^\alpha C_x' \xrightarrow{e} -4H_z^\alpha C_x^\alpha C_z' \xrightarrow{f} -2C_y^\alpha C_z'$$

where H^α, C^α, and C' represent the angular momentum operators for $^1H^\alpha$, $^{13}C^\alpha$, and $^{13}C'$ spins, respectively. Optimal values of delays *A*, *B*, *C*, and *D* in the sim-CT HMQC HA(CA)(CO)NH experiment (Figure 1) are uniquely determined by following equations

$$2\tau_a + A - B - C + D = t_1 \quad (1)$$

$$A + B - C - D = 0 \quad (2)$$

$$A + B + C + D + \tau_{a\_foc} = 2T_c \quad (3)$$

$$A - B + C - D = 0 \quad (4)$$

where eqs 1−4 are derived from the requirements of H^α frequency-labeling during the evolution time t_1, refocusing of C^α chemical shift evolution during t_1, constant-time evolution of carbon−carbon and proton−proton scalar couplings, and refocusing of heteronuclear two- and three-bond scalar couplings of H^α and C^α nuclei, respectively. The solutions for this set of equations are $A = D = T_c/2 + t_1/4 - \tau_a/2 - \tau_{a\_foc}/4$ and $B = C = T_c/2 - t_1/4 + \tau_a/2 - \tau_{a\_foc}/4$. The sim-CT HMQC pulse sequence shown in Figure 1 was designed to utilize a sufficiently large value t_{1max} to allow useful spectral resolution, where t_{1max} is given by $2T_c + 2\tau_a - \tau_{a\_foc}$.

These HSQC and sim-CT HMQC frequency-evolution periods were compared using samples of 124-residue $^{15}N,^{13}C$-enriched RNase A and 58-residue $^{15}N,^{13}C$-enriched BPTI proteins. Figure 2 shows H^N-H^α 2D spectra of RNase A at a temperature of 20 °C generated using the HSQC and sim-CT HMQC pulse sequences shown in Figure 1. It is clear that there are significant enhancements in signal intensities evident by overall stronger cross peaks in the sim-CT HMQC experiment compared with those in the HSQC version. Figure 3 shows several representative traces taken from the spectra shown in Figure 2. The sim-CT HMQC spectra exhibit narrower resonance line widths and enhanced peak intensities compared with those from the HSQC version of the experiment. The intensity enhancement factors for residues T36, C58, and I81 are 1.36, 1.36, and 1.47, respectively. Quantitative analyses of 86 cross peak intensities indicate that ~90% of the cross peaks exhibit an average of 23% enhancements, whereas ~10% of the cross peaks exhibit an average of 10% reduction in signal intensity (Figure 4A); quantitative analyses of 43 cross peak intensities of BPTI at a temperature of 10 °C result in a similar conclusion (Figure 4B). On average the sim-CT HMQC experiment exhibits ~20% enhancement compared with that obtained with the HSQC version (Figure 4).

The transverse relaxation rates of the single-quantum C^α coherences are mainly due to the dipolar relaxation between the C^α and its directly attached H^α. This interaction is eliminated in the multiple-quantum coherences. However, the dipolar interactions between these H^α nuclei and other protons that are nearby in three-dimensional structure contribute to the transverse relaxation rates of these multiple-quantum coherences. Thus, the observed sensitivity enhancement is a balance between the improved relaxation properties of $^1H-^{13}C$ MQ coherences over SQ ^{13}C coherences due to elimination of the relaxation contribution from the directly-bonded proton and the effects of local proton density on $^1H-^{13}C$ MQ relaxation rates; while for most $C^\alpha-H^\alpha$ sites in these proteins, the net effect is an enhanced sensitivity, for some sites the sim-CT HMQC experiment is actually somewhat less sensitive.

Signal intensities in the sim-CT HMQC experiment are also modulated by both carbon−carbon and proton−proton homonuclear scalar coupling interactions during the constant-time proton evolution period. Optimal values of the delay $2T_c$ determined by the set of carbon−carbon scalar couplings and relaxation effects were found to be around 8 ms. Proton−proton scalar couplings modulate the signal intensities as $\Pi_i \cos(2\pi J_{HHi} T_c')$ where $2T_c' = 2T_c + 2\tau_a - \tau_{a\_foc}$. For a non-glycine H^α with scalar coupling interactions, $^3J(H^\alpha-H^N) \approx 7$ Hz, $^3J(H^\alpha-H^{\beta 2}) \approx 4$ Hz, and $^3J(H^\alpha-H^{\beta 3}) \approx 12$ Hz and the coherence evolution periods $2T_c = 8.4$ ms, $\tau_a = 1.6$ ms, $\tau_{a\_foc} = 2.3$ ms, $\Pi_i \cos(2\pi J_{HHi} T_c') = 0.92$; i.e., the attenuation of

(25) Sørensen, O. W.; Eich, G. W.; Levitt, M. H.; Bodenhausen, G.; Ernst, R. R. *Prog. NMR Spectrosc.* **1983**, *16*, 163−192.

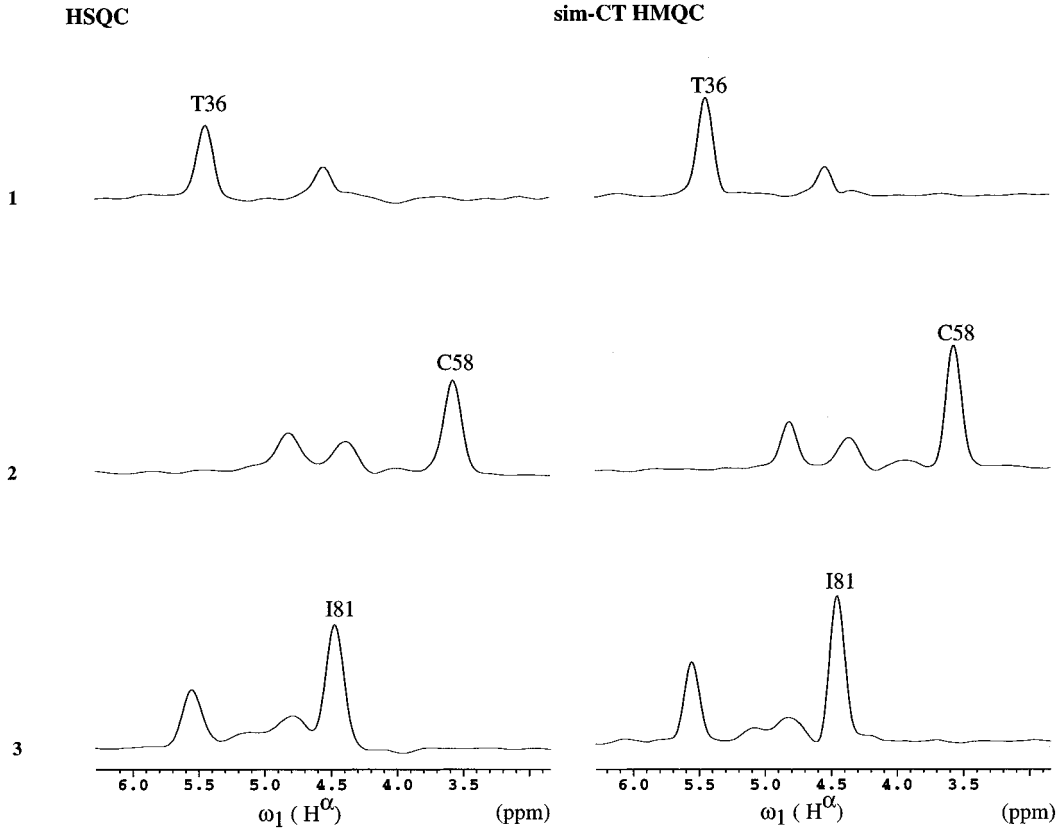

Figure 3. Comparison of traces along ω_1 for $H^{\alpha}_{i-1}(\omega_1)-H^{N}(\omega_3)$ 2D spectra of RNase A generated with the two HA(CA)(CO)NH pulse sequences of Figure 1. The traces were taken from Figure 2 as marked by arrows. Traces were plotted with same vertical scale setting and noise level.

HMQC due to the constant-time proton-proton homonuclear scalar coupling is ∼8%.

The simultaneous ^{1}H and ^{13}C constant-time multiple-quantum coherence scheme described in this study has several advantages: (i) incorporation of proton frequency evolution times into the constant-time period significantly minimizes the total length of the pulse sequence; (ii) utilization of multiple-quantum coherences generally prolongs transverse relaxation times of C^{α} coherences; and (iii) simultaneous constant-time evolution of homo- and heteronuclear couplings suppresses splittings of resonance in the indirect HMQC dimensions. The average enhancement of ∼20% in the sim-CT HMQC experiment is due to both utilization of the improved relaxation properties of multiple-quantum coherences[14−19] and concatenation of proton frequency evolution period into a constant-time period. Since the utilization of HMQC relaxation results in, on average, only ∼5% enhancement,[18] most of the ∼20% enhancement observed in the sim-CT HMQC experiment is due to the concatenation of the proton frequency evolution period into the constant-time period.

In addition, the resulting constant-time data sets are suitable for processing with mirror-image linear prediction[26] and 4D versions of the experiment with constant-time evolutions in three indirect dimensions can be readily obtained without extending pulse sequence length. The sim-CT HMQC proton evolution scheme described here significantly increases spectrum sensitivity as demonstrated in this study and is expected to give even greater enhancements in larger proteins with short $^{13}C^{\alpha}$ SQ

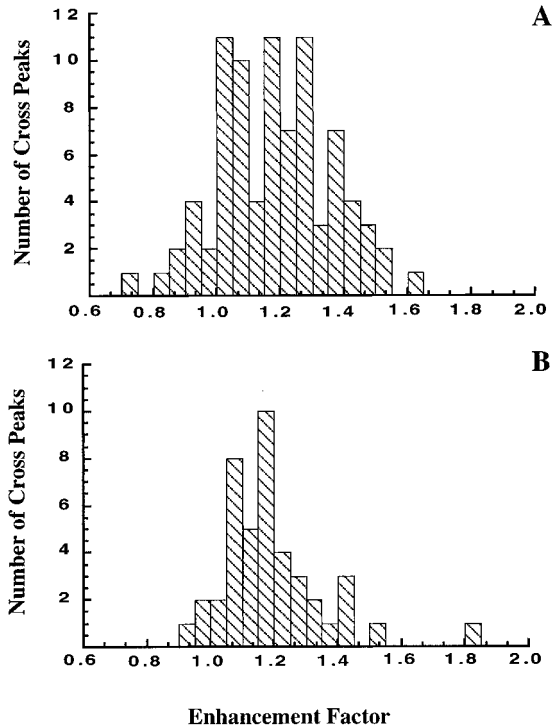

Figure 4. Histogram plots of the numbers of cross peaks vs enhancement factor (sim-CT HMQC:HSQC) measured in HA(CA)-(CO)NH spectra of (A) RNase A at 20 °C and (B) BPTI at 10 °C. The enhancement factor is defined as the ratio of cross peak average signal-to-noise ratios of the sim-CT HMQC and HSQC spectra. For these statistics, 84 well-resolved cross peaks were taken from the data set shown in Figure 2 for RNase A and 43 well-resolved cross peaks were taken from spectra for BPTI.

(26) Zhu, G.; Bax, A. *J. Magn. Reson.* **1990**, *90*, 405−410.
(27) Shaka, A. J.; Barker, P. B.; Freeman, R. *J. Magn. Reson.* **1985**, *64*, 547−552.
(28) Marion, D.; Ikura, M.; Tschudin, R.; Bax, A. *J. Magn. Reson.* **1989**, *84*, 393−399.
(29) Kay, L. E.; Keifer, P.; Saarinen, T. *J. Am. Chem. Soc.* **1992**, *114*, 10663−10665.

transverse relaxation times compared with HSQC-type experiments. This concept of sim-CT HMQC with concatenated proton evolution is quite general and can be applied for sensitivity enhancement in many other heteronuclear multidimensional correlation experiments.

Experimental Section

NMR spectra were collected on a Varian Unity 500 NMR spectrometer system equipped with three independent channels and a computer-controlled fourth synthesizer for carbonyl pulses and decoupling. NMR samples were prepared in Shigemi NMR tubes. These samples included uniformly ^{13}C,^{15}N-enriched RNase A at pH 4.6 and protein concentration of 2 mM, and uniformly ^{13}C,^{15}N-enriched BPTI at pH 5.8 and protein concentration of 2 mM. Data processing was carried out with Varian VNMR software.

Acknowledgment. We thank Ms. R. Watson for useful editorial comments on the manuscript. This work was supported by grants from the National Institutes of Health (GM-47014, GM-50733), the National Science Foundation (MCB-9407569), a National Science Foundation Young Investigator Award (MCB-9357526), and a Camille Dreyfus Teacher-Scholar Award. Support for computing facilities was provided by a grant from the W. M. Keck Foundation.

Supporting Information Available: Pulse sequences and decoupling wave forms for Figure 1 are available through the Internet only. See any current masthead page for ordering and Internet access instructions.

JA970734K